# A new hydride: $MgH_x$ prepared by ion implantation



1991 J. Phys.: Condens. Matter 3 8767

(http://iopscience.iop.org/0953-8984/3/45/002)

J. Phys.: Condens. Matter 3 (1991) 8767–8776. Printed in the UK

# A new hydride: $MgH_x$ prepared by ion implantation

H Köstler†, A Traverse‡, P Nédellec‡, L Dumoulin‡, M O Ruault‡, L Schlapbach†, J P Burger§ and H Bernas‡

† Physikalisches Institut, Universität Fribourg, CH-1700 Fribourg, Switzerland
‡ Centre de Spectrométrie Nucléaire et de Spectrométrie de Masse, CNRS-IN2P3, Bâtiment 104–108, F-91405 Campus Orsay, France
§ Laboratoire Hydrogéne et Défauts dans les Métaux, Bâtiment 350, F-91405 Campus Orsay, France

Received 17 June 1991

**Abstract.** A non-equilibrium Mg hydride was prepared by low temperature hydrogen implantation in Mg thin films. In contrast to the usual compound in which H is charged under high pressure and elevated temperature, no structural phase transformation from hexagonal to tetragonal is observed here. Implanted H atoms progressively fill the tetrahedral interstitial sites of the Mg hexagonal cell up to a concentration H/Mg around one. The resulting hydride is metallic whereas the classical $MgH_2$ is an insulator.

## 1. Introduction

The study of metal–hydrogen systems is of considerable interest in relation to basic properties (the stability of the hydrides, the change of the atomic and electronic structure) and possible applications such as hydrogen storage. The insertion of hydrogen can be obtained by electrolysis, by application of H pressure (Alefeld and Völkl 1978) but also by ion implantation (Traverse and Bernas 1987).

Because Mg is a light metal, the possibility of inserting large amounts of H can favour technical applications. Preparation of the dihydride $MgH_2$, which is an electrical insulator, occurs essentially at high temperatures ($T > 440\,^{\circ}C$) and high pressures ($p_{H_2} > 30$ atm) (Stampfer *et al* 1960) which indicates that this hydride is less stable than other dihydrides such as the rare earth ones for which $p_{H_2}$ is about $10^{-3}$ atm and the other saline hydrides i.e. $CaH_2$, $SrH_2$, $BaH_2$ (Mueller *et al* 1968). For these reasons, it is interesting to study the formation of $MgH_x$ in thin films by the implantation technique because the insertion of H can be done at low temperature. Measurements of the transport properties and of the lattice parameters as a function of $x$ may be performed. Previous H charging by implantation (Chami *et al* 1978) at 40 K achieved a low concentration of around 0.01: the H-site occupancy was identified as tetrahedral in the Mg hexagonal structure.

In the present work we checked the possibility of preparing magnesium dihydride by low-energy H implantation. Large and controlled amounts of H (up to $x = 3$) were introduced step-by-step so that the physical properties of the system might be followed at each stage of the formation process. Studying the samples by *in situ* Rutherford backscattering spectrometry (RBS) and *in situ* transmission electron microscopy

0953-8984/91/458767+10$03.50  

(TEM), we obtained information on the composition and structure. The resistance was monitored as the nominal H content increased. The implanted hydrogen profile is near-Gaussian but under certain energy conditions, the width at half maximum is broad enough to consider that the concentration is nearly homogeneous through the sample depth, a prerequisite for detecting a possible metal–insulator transition. The resistance was also measured during annealing to study the thermal stability.

Instead of forming the expected tetragonal dihydride, we ended up with a supersaturated solid solution of H in hexagonal Mg with a concentration ratio of H/Mg around one. There was no evidence of a metal–insulator transition.

## 2. Experimental details

For transport measurements and RBS experiments, thin Mg films (58 nm) were deposited either on quartz or carbon substrates by electron gun evaporation under a vacuum of $10^{-9}$ Torr. They were covered with a 57 nm thick evaporated SiO layer.

Hydrogen implantations were performed either at 80 K in conjunction with RBS experiments or at 6 K in conjunction with transport measurements. An incident energy of 4 keV was chosen so that, due to the energy loss in the SiO overlayer, the hydrogen profile in the Mg film is homogeneous. The implantation profile is approximately centred in depth in the middle of the Mg film (total $R_p$ = 75 nm (Ziegler *et al* 1986) with a straggling of 28 nm. Under these conditions, a fluence of $3 \times 10^{17}$ H cm$^{-2}$ roughly corresponds to $x$ = H/Mg of one. Fluences as high as $9 \times 10^{17}$ were implanted.

RBS spectra were recorded between implantations steps at 80 K for H/Mg ratios of 0, 1 and 2 with 1 and 2 MeV He incident particles. The resistance was measured between increasing steps of H fluence at 4.2 K. At some fluence steps, the time dependence of the resistance was followed for several minutes. At H/Mg ratios of 0, 0.05, 0.15, 0.3, 0.7, 1.5 and 3, we also recorded the Hall voltage at 4.2 K, and the magnetoresistance under a perpendicular field of 4 T at different temperatures (from 1.4 up to 10 K). Results for the Hall voltage and magnetoresistance will be presented in a later article. The resistance temperature dependence on $x$ was followed between 1.4 and 20 K. Some of these measurements were performed just after implantation while others were taken after annealing at $T$ = 20, 50 or 115 K.

The resistances of the samples with H/Mg = 0.3, 0.7, 1.5, 3 were measured during annealing up to 300 K then during cooling to 4 K before a second series of anneals and measurements up to room temperature.

For *in situ* TEM observations, we implanted 11 keV hydrogen ions in a polycrystalline Mg thin film (thickness about 170 nm) cooled to 15 K. The angle between the sample and the ion beam was set at 45°. In order to avoid ion beam heating effects, the dose rate was fixed at $2 \times 10^{13}$ H cm$^{-2}$ s$^{-1}$. The implantation was carried out step-by-step ($0.4–1 \times 10^{17}$ H cm$^{-2}$) alternating with TEM observations. The highest implanted fluence was $9.2 \times 10^{17}$ H cm$^{-2}$. From TRIM simulations (Ziegler *et al* 1986), two doped regions were defined: from $\sim$ 50 to $\sim$ 140 nm there is a fairly homogeneously doped region; outside this zone, considerable H inhomogeneity prevails. Since, by means of electron microscopy, we observe the projection of both regions, the prevalently observed variation is due to the highest doped region. In the latter, an implantation step of $10^{17}$ H cm$^{-2}$ roughly corresponds to $x$ about 0.2.

A hydrogen profiling experiment was performed at room temperature on samples implanted at 80 K with $x$ = 2 using the $N^{15}(H, \alpha\gamma)\ C^{12}$ resonant nuclear reaction

at an energy of 6.35 MeV for the $N^{15}$. Optical microscopy observations and scanning electron microscope (SEM) microprobe analysis were also performed on samples after their implantations and annealing up to 300 K.

All these experiments, except the SEM ones, were performed on the transmission electron microscope, IRMA implanter and ARAMIS accelerator of the CSNSM (Cottereau *et al* 1989).

## 3. Results

### *3.1. TEM observations*

Before implantation, two types of crystal exhibiting significant epitaxial orientations were selected. Some large hexagonal crystals (of the order of 1 $\mu$m; see figure 1(*a*)) showing a (0001) basal plane and electron diffraction pattern (EDP (figure 1(*b*)), and smaller crystals (about 0.1 to 0.4 $\mu$m; figure 2(*a*)) exhibiting a (2110) basal plane with two main perpendicular epitaxial orientations (the corresponding EDP is displayed in figure 3(*a*)). The structural evolution was followed in these two most significant regions.

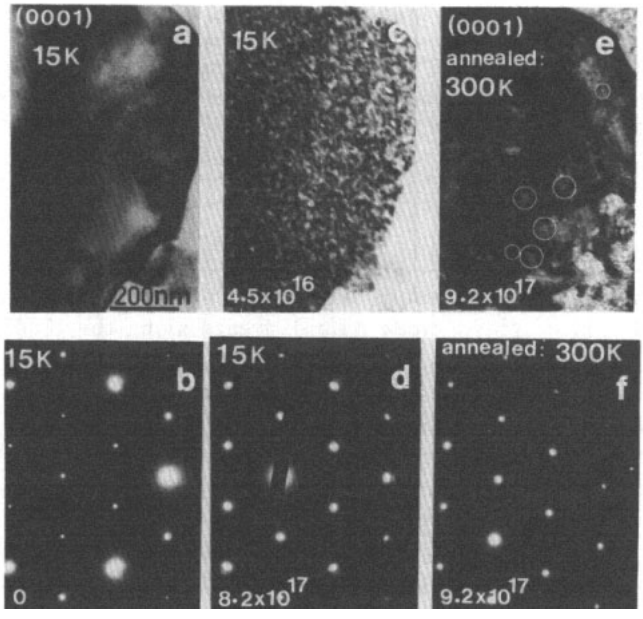


**Figure 1.** A (0001) crystal implanted at 15 K with H ions at 11 keV: (*a*), (*b*) bright field and corresponding EDP before implantation; (*c*) bright field showing dislocation loops at the first step of the implantation ($\sim 4.5 \times 10^{16}$ H cm$^{-2}$); (*d*) EDP at a high doping level (H/Mg about 1.6 i.e. $8.2 \times 10^{17}$ H cm$^{-2}$) showing no superstructure formation from a new phase; (*e*),(*f*) bright field and EDP after $9.2 \times 10^{17}$ H cm$^{-2}$ implantation and thermal annealing at 300 K. We observe some hexagonal-shaped voids inside the crystal as indicated by circles.

Dislocation loops induced by H implantation were observed (figure 1(*c*)) after the first fluence (i.e. $\sim 4.5 \times 10^{16}$ H cm$^{-2}$). No structural change (figures 1(*b*), (*d*), (*f*) was observed in the (0001) basal plane up to the maximum fluence (e.g. $9.2 \times 10^{17}$ H cm$^{-2}$).

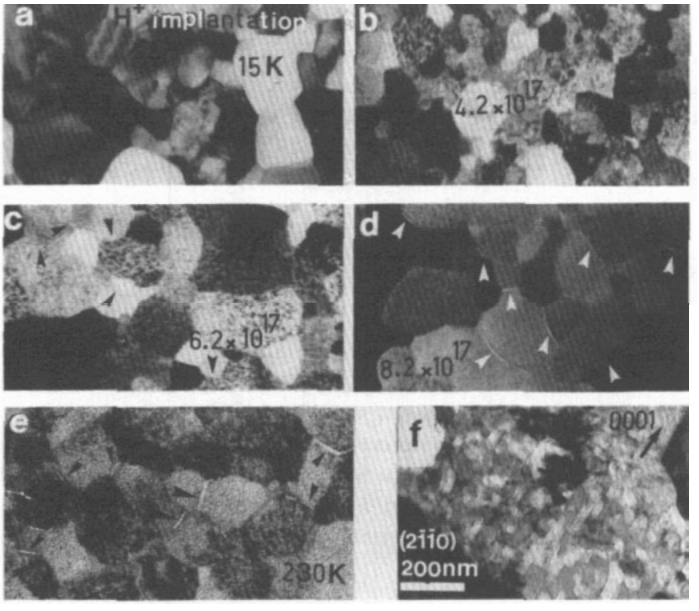


**Figure 2.** A (2110) Mg polycrystalline region implanted at 15 K with H ions at 11 keV: bright fields (*a*) before implantation; (*b*) at $\sim 4 \times 10^{17}$ H cm$^{-2}$; (*c*), (*d*) from $\sim 6 \times 10^{17}$ H cm$^{-2}$ (they show some grain boundary modification, indicated by arrows); (*e*), (*f*) during thermal recovery from 15 to 300 K showing bubble (or void) formation from 230 K which are superimposed and exhibit a faceted shape at 300 K.

These observations exclude $MgH_2$ precipitation in our samples. This is in contrast to the results obtained on high-pressure charged samples (Shober and Chason 1982).

In the (2110) basal plane, weak diffuse streaks along the ⟨0001⟩ directions appeared above a fluence of $\sim 3 \times 10^{17}$ H cm$^{-2}$ (figure 3(*b*)) and the spots extended along the ⟨0001⟩ directions. They are reinforced by increasing H-implantation fluences (figure 3(*d*)). This indicates that, due to the H implantation, there is at least an asymmetric disorder leading to strain along the *c*-axis, but without any significant modification of the lattice parameters of Mg. Simultaneously above $\sim 6 \times 10^{17}$ H cm$^{-2}$ (e.g. $x \approx 1.2$), a contrast change of some grain boundaries is observed presumably due to H diffusion towards the grain boundaries. A similar phenomenon was observed in H-doped polycrystalline TiC (Fournier *et al* 1987). It was related to the grain boundary amorphization due to H accumulation. In the present case, whether or not the grain boundaries are amorphized is not resolved.

During thermal annealing up to 300 K (figures 1(*e*), (*f*), 2(*e*), (*f*) and 3(*d*), (*f*)) the disorder along the c-axis was enhanced until $\sim$ 140 K and we observed, at 300 K, the undoped structure in the EDP. In addition, a few small spots came from MgOH phase formation and extra weak streaks are due to (002) MgO double diffraction on the superimposed faceted voids. The voids appear in fact at $\sim$ 200 K (figure 2(*d*)) and increase until they are faceted and superimposed at 300 K. The latter exhibit a rectangular shape along ⟨0001⟩ in the (2110) plane and are hexagonal in the (0001) plane and their density is orientation-dependent ($\sim$ 10 times lower in the (0001) than in the (2110) basal plane).

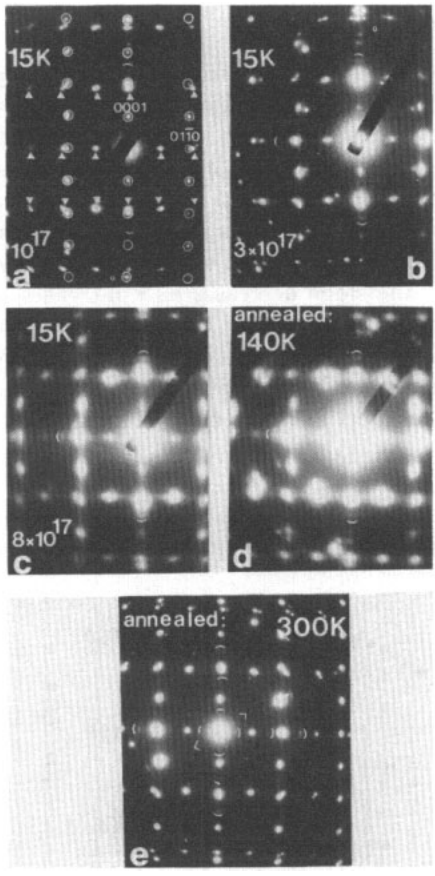


**Figure 3.** (*a*) Typical EDP obtained in (2110) Mg polycrystalline regions. We observe two main perpendicular epitaxial orientations. The circled one is indexed and the other is indicated by arrows. Some weak streaks (underlined by a circular arc) from MgO are often observed. (*b*), (*c*) EDP evolution during implantation. Since $3 \times 10^{17}$ H $cm^{-2}$ streaks along the (0001) directions appear in each figure and the spots extend along the latter. (*d*), (*e*) During further thermal annealing, the intensity extension is enhanced until ~120 K. At 300 K the initial EDP is recovered. In addition, we observe small spots from MgOH and some small and weak streaks coming from MgO multiple diffraction presumably due to the faceted void presence.

### *3.2. RBS measurements*

Before H implantation, a low level of oxidation (less than 6%) was measured through RBS on Mg thin films deposited on carbon without any sublayer. Oxygen was mainly located at the carbon interface and at the sample surface. Hence samples covered with SiO might contain even less oxygen. Comparison between experimental spectra (not shown here) taken at 80 K, for H/Mg = 0, 1 and 2, and theoretical spectra calculated using the RUMP code (Doolittle 1985) showed that both width and height modification of the Mg peak is well reproduced when going from H/Mg = 0 to 1, while the discrepancy is large for H/Mg = 2. A spectrum recorded after annealing up to 300 K is also different from the one calculated assuming pure Mg. Optical microscopy and SEM microprobe analysis performed on a sample with H/Mg = 2 annealed up to 300 K revealed cracks and blisters located in the SiO layer.

### *3.3. Resistance fluence dependence*

The residual resistive ratio of four testifies to the purity of our Mg samples, as does the low oxygen amount determined by RBS. The resistance measured at 4.2 K is plotted against the H fluence in figure 4. A resistivity scale is also provided on the right-hand side of the figure. Up to $x = 3$, no sign of a resistance divergence is seen in contrast to the prediction of an insulator transition. In the low concentration range, around 0.001, a slope of about 10 $\mu\Omega$ cm/1% of H was measured which does not appear on the figure. After a resistance increase with a slope of about 1 $\mu\Omega$ cm/1% of H in the concentration range up to $x = 1$, the slope decreases as $x$ increases to $x = 3$ with a tendency to saturation. In order to check whether the resistance saturation was due to some inhomogeneities in the H profile leading to more conducting paths in parallel with the insulating ones, we changed the H incident energy. This did not induce any resistance increase as shown in the insert in figure 4.

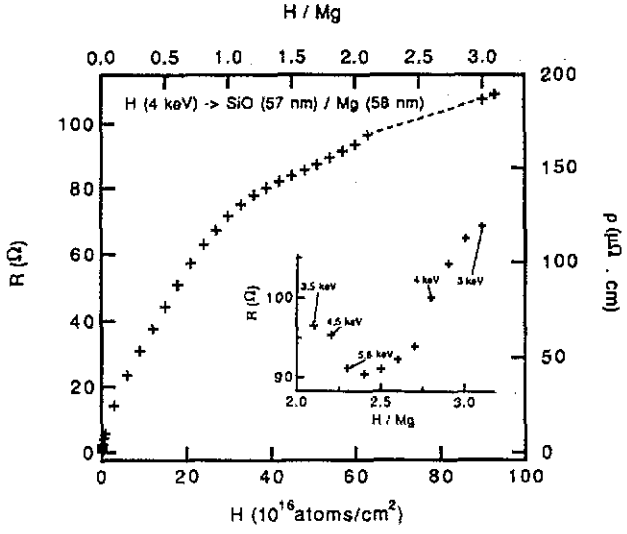


**Figure 4.** Resistance fluence dependence for H implanted at 4.2 K in Mg. In the insert the behaviour of $R$ during H incident energy changes is displayed.

A resistance minimum after a slope decrease had been observed in implanted PdH at an H/Pd ratio of about 1, due to the filling of the octahedral sites of the cubic lattice (Traverse and Bernas 1987). A resistance minimum at H/Mg = 2 could have indicated complete ordering in the tetrahedral interstitial sites of the Mg structure. No such minimum was observed. Hence the slope decrease above H/Mg = 1 cannot be interpreted as a precursor effect of such ordering. It is more likely related to H migration towards grain boundaries or the sample surface as demonstrated by TEM and RBS.

### *3.4. Resistance temperature dependence*

At temperatures as low as 1 K the resistance was found to decrease systematically as a function of time with a (log $t$) law. This variation of small amplitude is plotted on figure 5 for a sample at 4.2 K; it is interpreted as a relaxation process of the implanted hydrogen.

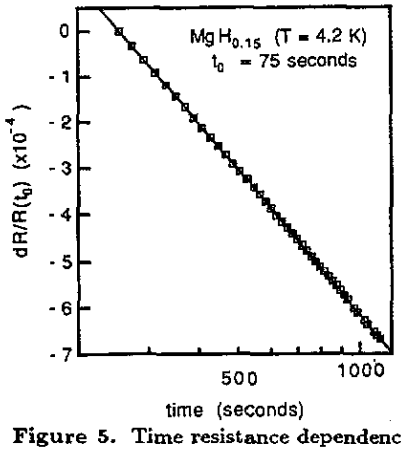


**Figure 5.** Time resistance dependence for a sample implanted at a concentration H/Mg = 0.15 measured at $T$ = 4.2 K.

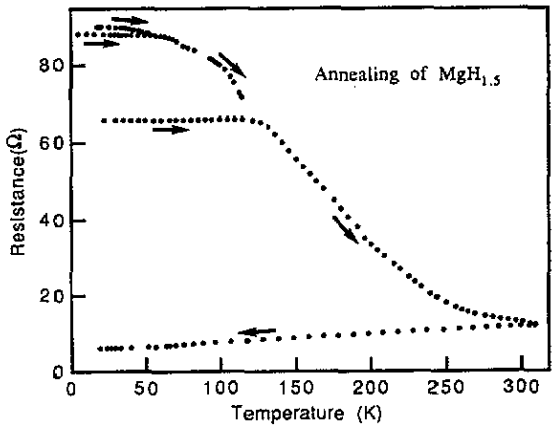


**Figure 6.** Temperature resistance dependence of a sample with H/Mg = 1.5 from 4.2 up to 300 K.

Samples were also very unstable as checked by the resistance temperature dependence. Typical resistance decreases after annealing up to 20 or 50 K were of the order of 3% while for annealing up to 115 K the resistance decrease was between 20% to 30%. A typical resistance behaviour measured from 4 up to 300 K is reported on figure 6 for H/Mg = 1.5. The main decrease observed above 140 K might correspond to H motions either out of the sample or towards grain boundaries. Indeed the nuclear reaction analysis performed after room temperature annealing provided an H/Mg ratio of 0.4 remaining in the target. Although a large resistance decrease was noticed after annealing up to 300 K, the initial resistance of the Mg films was not recovered (at 4.2 K, 5 Ω after implantation and annealing instead of 0.5 Ω for pure Mg).

## 4. Discussion

### *4.1. The Mg dihydride is not formed*

TEM observations clearly demonstrate that H absorption by Mg through low temperature implantation does not lead to the equilibrium tetragonal magnesium dihydride.

The diffraction pattern displayed neither the spots typical of $MgH_2$ nor any indication of another structural transformation. Other less direct evidence in the same direction is:

(i) the resistance did not diverge as expected if a metal–insulator transition occurred;

(ii) above 140 K hydrogen implanted at 4 K was seen to move out of the Mg lattice and at $T = 300$ K a major part of the H has left the sample whereas the magnesium dihydride is stable at room temperature;

(iii) from the experimental RBS spectrum at $x = 2$ for an implantation at 80 K, it is clear that a significant proportion of H has already desorbed.

All these behaviours suggest that the non-formation of $MgH_2$ is due to the absence of a transformation from a hexagonal to a tetragonal structure. A similar absence of a phase transformation has been observed in previous experiments on low temperature implanted NbH (Lin *et al* 1987). Hence, these two results indicate that low temperature implantation does not favour the structural phase transformation.

### *4.2. What did we form?*

From previous results obtained on hydrogen implanted in Mg (Chami *et al* 1978), it is known that protons occupy the tetrahedral interstitial sites for $x$ of the order of 0.01. In other systems (Ni, Pd, Ag etc (Traverse and Bernas 1987)), we have shown that implantation proceeds in a random occupancy of the interstitial sites even at high concentrations. We suggest that in the case of $MgH_x$, implanted protons randomly occupy the tetrahedral sites of the Mg hexagonal cell, leading to the formation of a supersaturated alpha phase. However, distances between the tetrahedral sites are $d_1 = 0.13$ nm for nearest neighbour sites located along the $c$-axis, $d_2 = 0.27$ nm for sites located in the $(abc)$ planes. According to the Switendick criterion (Switendick 1978), two hydrogens cannot stay at a distance less than 0.21 nm without the lattice being modified. In the case of Mg, this leads to a maximum concentration of 1. Note that the RBS spectra are in agreement with a filling to H/Mg = 1. In fact even around $x = 0.6$, stress induced by H implantation was seen on diffraction patterns; at higher concentrations, H migrated towards grain boundaries or to the sample surface as evidenced on TEM pictures and on the resistance against fluence saturation.

### *4.3. Stability of the system*

It is well known that the stability of H is related to the formation of metal–hydrogen bonding bands occurring at low energy because of the strong proton potential. These bonding bands involve electrons of the metal whose energy is lowered so that it favours the H solubility; but a fraction of the supplementary electrons brought by H is often added to the Fermi surface, a fact which does not favour H stability. One can mention *a priori* that H in hexagonal metals is never very stable. This is true for instance in all hexagonal rare earth metals. Our results indicate that the implanted $MgH_x$ is highly unstable as seen from the resistance variation either with time or temperature. H occupancy of the tetrahedral interstitial sites in the hexagonal cell does not favour the formation of the corresponding H–metal bonding bands above $x = 1$. In contrast, in tetragonal $MgH_2$, H occupies the octahedral-like interstitial sites for which apparently the bonding bands form very well.

### *4.4. Transport properties*

At very low fluences, $10^{13}$ H cm$^{-2}$, the resistance and H content relationship is due to electron scattering both on H and implantation-induced defects. A slope of the order of 30 $\mu\Omega$ cm/1% of H is expected corresponding to about eight Frenkel pairs per incident H times 4 $\mu\Omega$ cm/%, the resistive contribution of a Frenkel pair in Mg (Lucasson 1975) and the pure H resistive contribution (Bernas and Traverse 1982). At fluences equal to $10^{14}$ H cm$^{-2}$ where we started our measurements, the saturation of the defect resistive contribution leading to a resistive slope of 10 $\mu\Omega$ cm/1% of H had already started.

For fluences of the order of $10^{16}$ H cm$^{-2}$, corresponding to H/Mg ratios of a few percent, defect saturation is reached and the slope decreased to values of the order of 1 $\mu\Omega$ cm/1% of hydrogen. This is the usual value observed in low concentration hydrides whatever the charging process, implantation or classical techniques such as hydrogen pressure or electrolysis. Each proton located on its interstitial site acts as an electron diffuser leading to the resistance increase. For H/Mg = 0.7, the resistivity is 97 $\mu\Omega$ cm, a large value which can be explained if each hydrogen continues to contribute individually to the electron scattering even at such high concentrations. We have already observed such a behaviour in amorphous implanted hydrides (Traverse *et al* 1984).

No divergence of the resistance against fluence curve is measured around H/Mg = 2, even after a change of the H incident energy, which indicates that the band structure of the system is different from that of the stable $MgH_2$. Neither lower energies nor higher ones induced the expected modification of the slope; higher energies even induced a resistance decrease interpreted as due to H precipitation towards grain boundaries for example.

## 5. Conclusions

We have prepared a new Mg hydride by low-temperature ion implantation. This highly unstable system is a supersaturated alpha phase in which the hexagonal structure of Mg remained unchanged with nearly no modification of the lattice parameters. Protons occupied tetrahedral interstitial sites but a complete filling of these sites was not possible as some of them are too close. The $MgH_2$ compound was never reached. The electronic band structure of the present hydride is thus different from that of the equilibrium Mg dihydride and no metal–insulator transition was observed. High resistivities are measured relating to electronic localization as will be shown in a forthcoming article reporting on magnetoresistance measurements and temperature resistance dependence in the low temperature range.

## Acknowledgments

We thank O Kaitasov for hydrogen implantations, R Laval for SEM observations. The Fribourg group acknowledges financial support from NEFF of Switzerland.

## References

Alefeld G and Völkl J (ed) 1978 *Hydrogen in Metals (Topics in Applied Physics 28)* (Berlin: Springer)

Bernas H and Traverse A 1982 *Appl. Phys. Lett.* **41** 245
Chami A C, Bugeat J P and Ligeon E 1978 *Radiat. Eff.* **37** 73
Cottereau E, Camplan J, Chaumont J and Meunier R 1989 *Mater. Sci. Engrg* B **2** 217
Doolittle L R 1985 *Nucl. Instrum. Methods* B **9** 344
Fournier D, Ruault M O and Saint Jacques R G 1987 *Nucl. Instrum. Methods* B **19/20** 559
Lin X W, Ruault M O, Bernas H and Traverse A 1987 *J. Phys. F: Met. Phys.* **17** 2179
Lucasson P 1975 *Int. Conf. on Fundamental Aspects of Radiation Damage in Metals (Gatlinburg, TN)* ed D T Robinson and F W Young p 42
Mueller W M, Blackledge J P and Libowitz G G 1968 *Metal Hydrides* (New York: Academic)
Shober T and Chason M K 1982 *Metal-Hydrogen Systems* ed T N Veziroglu (Oxford: Pergamon) p 177
Stampfer J F, Holley C E and Suttle T F 1960 *J. Amer. Chem. Soc.* **82** 3505
Switendick A C 1978 *Hydrogen in Metals (Topics in Applied Physics 28)* ed G Alefeld and J Völkl (Berlin: Springer) p 101
Traverse A and Bernas H 1987 *J. Less Common Met.* **129** 1
Traverse A, Bernas H, Chaumont J, Fan X J and Mendoza-Zelis L 1984 *Phys. Rev.* B **30** 6413
Ziegler J F, Biersack J P and Littmark U 1986 *The Stopping and Range of Ions in Solids* (New York: Pergamon)